J Mater Sci (2006) 41:4965–4969
DOI 10.1007/s10853-006-0127-3

LETTER

Dilatometric measurement of carbon enrichment in austenite during bainite transformation

Smati Chupatanakul · Philip Nash

Received: 2 November 2005 / Accepted: 6 March 2006 / Published online: 13 May 2006

The bainite transformation in steels can provide improved mechanical properties over tempered martensite microstructures [1]. For some components such as gears, a bainitic surface structure with a tempered martensite core provides optimum properties. In order to obtain such a distribution of microstructures, it is necessary for the component to be case carburized. This provides the opportunity to austemper at a temperature, which is above the M_S of the surface region to allow transformation to bainite but below the M_S of the core so that a tempered martensite structure is produced. Since case carburization leads to a carbon concentration gradient decreasing away from the surface the bainite transformation kinetics vary with distance. In order to optimize the processing, it is necessary to understand how carbon content affects the bainite transformation kinetics. Bainite transformation kinetics can be determined by dilatometry. Although dilatometry has been used to measure M_S temperature during bainite transformation [2], the measurements were not made as a function of bainite transformation time and were not correlated to carbon content in the austenite. In this work, we have established the carbon content in austenite as a function of austempering time by dilatometry.

The carbon concentration of bainitic ferrite during transformation is one of the most important factors to determine and understand the kinetics of carbide precipitation during the bainite transformation. It is widely believed that there is initially a shear transformation of austenite to ferrite of the same carbon content which is followed by the carbon supersaturation in bainitic ferrite being relieved under paraequilibrium boundary conditions by partition into the residual austenite during the bainite transformation and by precipitation of carbon [3–9]. An alternative model has been considered in which the carbon diffuses during the transformation of austenite to ferrite under equilibrium condition at the interface [3–6]. A third model intermediate between the other two has been considered in which the ferrite grows with a partial supersaturation of carbon and the remaining carbon partitioning into austenite or forming carbides [3–6, 8, 10–13]. These different models predict different limiting carbon contents in the austenite before the transformation ceases.

In this work, we are interested in the transformation kinetics in the carburized case of a 4317M2 steel. In order to study the transformation kinetics in the case two experimental heats with carbon contents of 0.58% and 0.82% were produced, Table 1, designated 2358 and 2359. These carbon contents correspond to the mid-point and maximum in the carbon case profile, respectively. The M_S temperatures of the steel 4317M2 and the two experimental heats were determined by dilatometry using the temperature profiles as shown in Fig. 1a). The first cycle is for the initial microstructure preparation. The second cycle is to identify the M_S temperature. Cylindrical specimens were machined with dimensions 10 mm diameter and 84 mm length and mounted in a Gleeble 3500 thermomechanical simulator and a diametrical dilatometer attached. The dilatometer was used to measure the diameter change during the thermal processing. The cooling rate used was the fastest cooling rate available in the Gleeble (i.e. continuous free cooling with power off), which is adequate to avoid the pearlite and bainite transformation regions in these steels. The dilatometry curve to determine the M_S temperature measured for 2358 is shown in Fig. 1b. It

S. Chupatanakul (✉) · P. Nash
Thermal Processing Technology Center, IIT, 10 W 32nd Street, Chicago, IL 60616, USA
e-mail: chupsma@iit.edu

Table 1 Chemical composition of the steels

	C	Mn	P	S	Si	Ni	Cr	Mo	Cu	Sn	Al	V	Nb	Ti
4317 M2	0.18	0.8	0.011	0.022	0.09	1.67	0.56	0.71	0.14	0.007	0.021	0.003	0.014	0.002
2358	0.58	0.82	0.004	0.023	0.04	1.9	0.55	0.77	0.04	–	0.028	–	–	–
2359	0.82	0.86	0.003	0.024	0.04	1.9	0.55	0.76	0.04	–	0.031	–	–	–

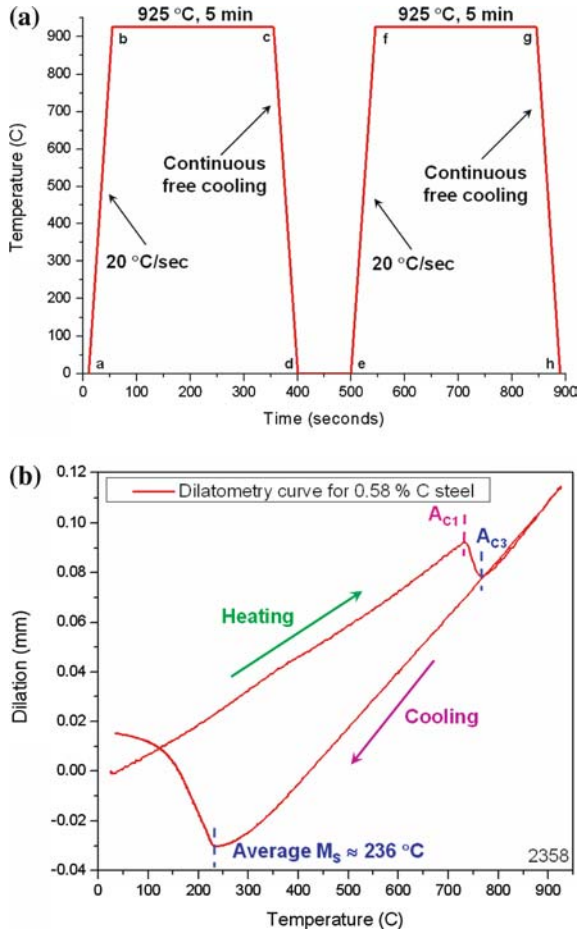

Fig. 1 M_S temperature determination; (**a**) temperature-time profile for 2358 and (**b**) dilatometry curve

shows the austenite begins to transform to martensite (the changing dilation) at 236 °C during cooling from the austenitizing temperature (925 °C) to room temperature (25 °C). The M_S temperatures were determined from the change in slope of the dilatometry curve on cooling. From the M_S temperatures measured for all three materials, which have essentially the same chemical composition except for carbon, we can obtain the relationship of M_S temperature as a function of carbon content, shown in Fig. 2 with the polynomial fit shown in Eq. (1) and Wang exponential dependency equation [14]:

$$M_S = 486.4 - 501.9(\text{wt\% C}) + 122.6(\text{wt\% C})^2 \quad (1)$$

The M_S temperature decreases as the carbon content in austenite increases. Using Eq. (1), we can calculate the carbon content for an M_S temperature corresponding to room temperature (25 °C) which is 1.39 wt% C and Eq. (1) is assumed to be valid up to this carbon content.

Austempering experiments were performed in order to measure the M_S temperature change as a function of austempering holding time. The austempering experiments for 2358 were performed in two cycles as shown in Fig. 3. The first cycle is to provide the same microstructure prior to each experiment. The second cycle is the austempering experiment to form bainite above the M_S temperature. The average austenite grain size for the austempering experiment was about ASTM 9.6 determined from several experiments. After completing the first cycle, the specimens were heated to austenitizing temperature (925 °C), held for 5 min and then cooled to different austempering temperatures (i.e. 300 °C and 340 °C). The specimens were held at the austempering temperature for different times and then cooled to room temperature (25 °C). The M_S temperature was measured for each different austempering holding time and austempering temperature during the cooling. Figure 4 shows the dilatometry result for the 0.58% C alloy austempered at 300 °C for 15 min. It can be seen that prior to the austempering there are no other transformations during cooling, confirming that the cooling rate is sufficient to avoid the pearlite nose of the C curve of the TTT diagram. There is a decrease of the M_S temperature upon austempering the material as a function of time. This decrease of M_S temperature is due to the rejection of carbon from bainite into austenite. Figure 5 shows the results of M_S temperature as a function of holding time for austempering temperatures of 300 °C and 340 °C. Each data point represents the average of at least three measurements. The measured M_S temperature represents the minimum carbon content in the austenite.

Austenite carbon content was calculated by taking the M_S temperature data as a function of austempering time and using Eq. (1). Figure 6 shows the relationship of the carbon content in austenite as a function of holding time. Upon austempering at 300 °C and 340 °C, there is an increase in carbon content in the austenite due to rejection of carbon from the bainite. However, the austenite carbon content reaches a limiting value, depending upon the austempering temperature, of about 1.32% C and 1.2% C for 300 °C and

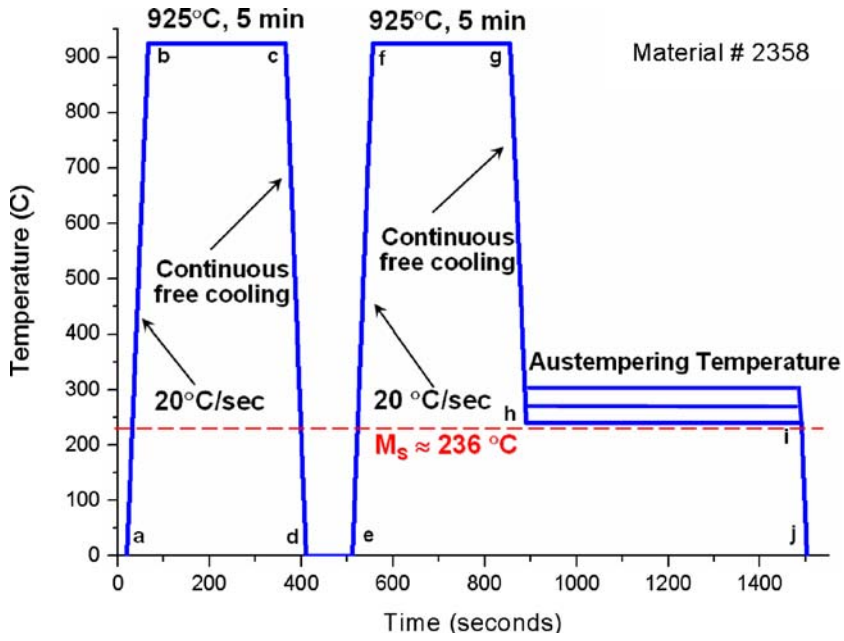

Fig. 2 Austempering experiment temperature–time profiles for steel 2358

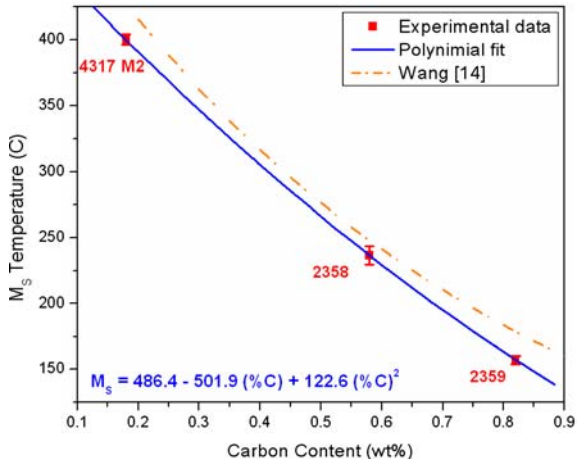

Fig. 3 M_S temperature as a function of carbon content

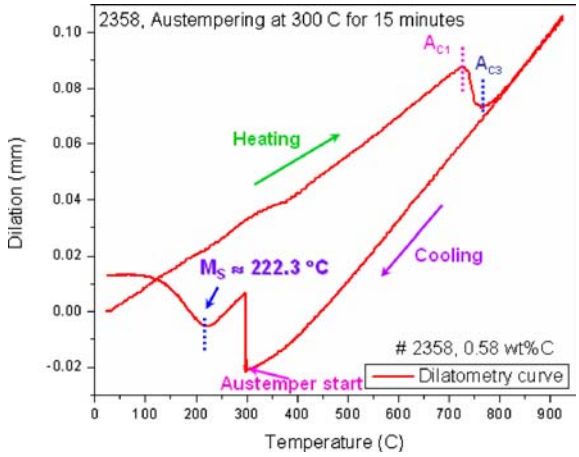

Fig. 4 M_S temperature measurement using dilatometry curve after austempering at 300 °C for 15 min

340 °C, respectively. As expected, the carbon rejection rate is higher at higher austempering temperatures.

In this work, the calculated carbon content in austenite assumes paraequilibrium i.e. only carbon is partitioned during the bainite transformation. If other elements partition, they will alter the M_S temperature. The chemical composition of austenite was predicted by assuming the bainite grows without any initial diffusion, so that some of the excess carbon is partitioned into the residual austenite and some as carbide precipitates. Quidort [15] showed carbon enrichment in austenite only in the region of the bainite laths because cementite precipitation removed the excess carbon. In our case we observe both carbide precipitation in the bainite laths and significant austenite carbon enrichment.

The transformation from austenite to bainite of the same composition has a thermodynamic driving force as long as the austenite has a higher free energy than the ferrite [3, 5, 6]. Ignoring the small term strain energy associated with the growth of bainite [3], the carbon content corresponding to T_0 at the austempering temperature, T_A, will define the limit for the lower bainite transformation. T_0 is the temperature at which austenite and ferrite of identical composition have equal Gibbs free energy and there is zero driving force. Once the austenite carbon concentration has reached that corresponding to the T_0 for that particular austempering temperature the transformation ceases. The bainite transformation cannot proceed if the carbon content of the austenite is beyond that corresponding to T_0 [3, 5, 6, 16, 17]. This reaction is said to be incomplete, since the

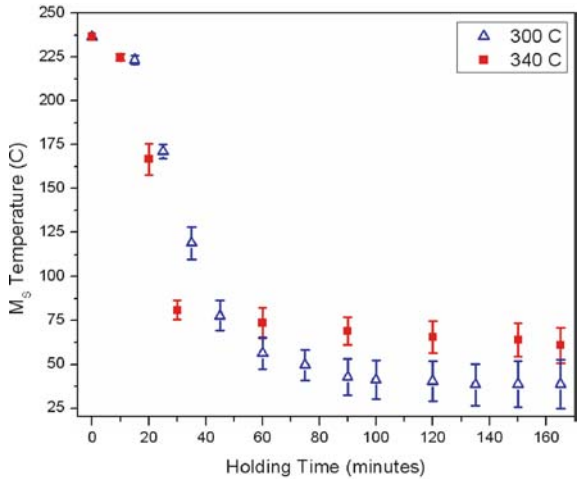

Fig. 5 M_S temperature as a function of austempering holding time

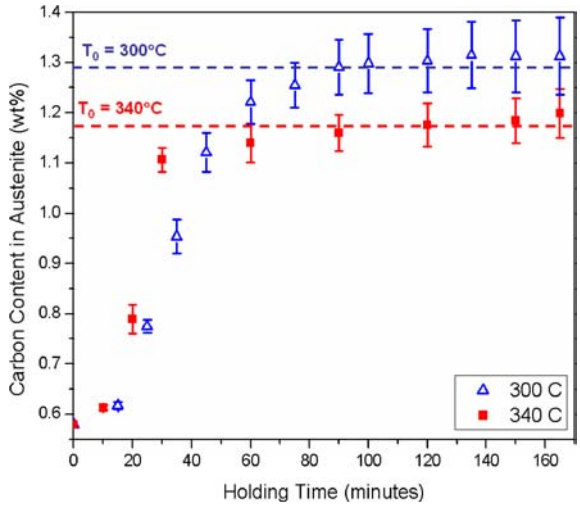

Fig. 6 Carbon content in austenite as a function of austempering holding time with calculated T_0 composition at each austempering temperature

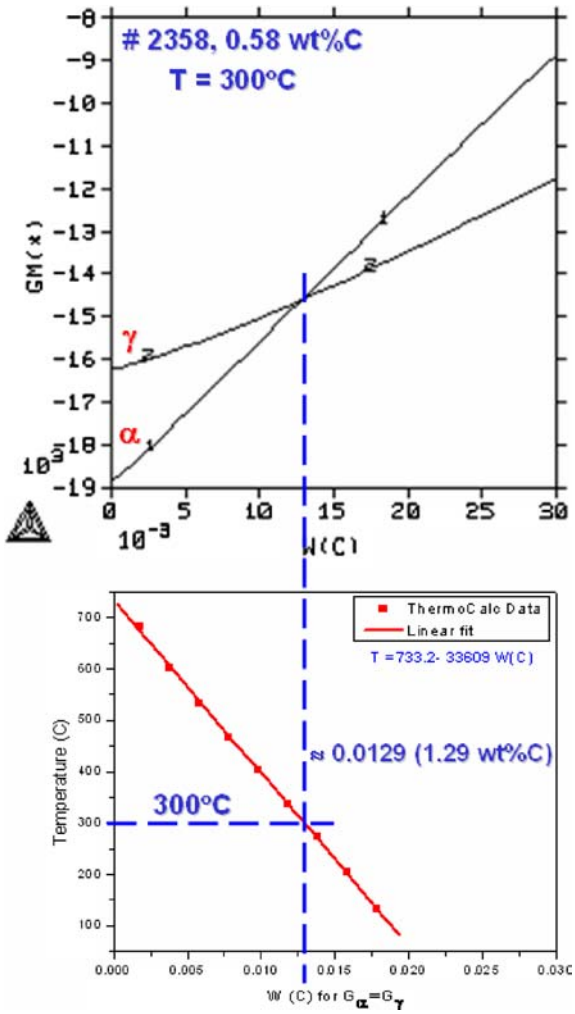

Fig. 7 Calculated free energy curves for ferrite and austenite and T_0 for 2358 at 300 °C

austenite has not achieved its equilibrium composition (given by the Ae_3 curve) at the point the reaction stops [3, 5, 6, 18, 19].

In order to ascertain if the limiting carbon content measured experimentally corresponds to the composition at T_0, free energy curves for ferrite and austenite in 2358 were calculated as a function of carbon content using Thermo-Calc™, Fig. 7(a). The T_0 calculation plot is shown in Fig. 7(b) and a linear fit to the data gives:

$$T_0 = 733.2 - 33609W(\mathrm{C}) \quad (2)$$

The carbon composition for T_0 is given in weight fraction of carbon ($W(C)$). From the above equation the carbon compositions corresponding to T_0 of 300 °C and 340 °C, are 0.0129 (1.29 wt% C) and 0.0117 (1.17 wt% C) respectively. The limiting carbon contents corresponding to $T_A = T_0$ are compared with the experimental results in Fig. 6. It is clear that there is excellent agreement between the measured limiting austenite carbon content achieved during the bainite transformation and the calculated carbon content corresponding to T_0.

In summary, the carbon content in residual austenite during the transformation to bainite at constant temperature was determined as a function of time by using the relationship between M_S temperature and carbon content as shown in Fig. 2 and Eq. (1). There is a good agreement between our experimental results and the exponential dependency equation of Wang [14]. During the bainite transformation, the carbon content in the residual austenite increases with increase of austempering holding time. The carbon content in austenite determined from measured M_S temperature represents the minimum carbon content in the residual austenite. The maximum values of carbon content obtained in the residual austenite from our experiments

show excellent agreement with the values of carbon content corresponding to $T_A = T_0$ calculated from Thermocalc™. These experimental results directly support the model of formation of fully supersaturated bainitic ferrite with the same composition as the austenite from which its for M_S followed by partitioning of carbon from ferrite to austenite and carbide precipitate in the ferrite laths. The transformation ceases after the carbon content in the austenite reaches the T_0 composition at the austempering temperature.

Acknowledgements The authors wish to thank Mr. R. Binoniemi of Dana Corporation for helpful discussions, provision of material and financial support of this project. The first author is also grateful to TPTC for the provision of a Finkl Fellowship.

References

1. Garcia -Mateo C, Caballero FG, Bhadeshia HKDH (2005) Mat Sci Forum 500–501:495
2. Lawrynowicz Z (2002) Mat Sci Tech 18:1322
3. Bhadeshia HKDH (2001) Bainite in Steels. The Institute of Materials, London, UK
4. Speer JG, Edmonds DV, Rizzo FC, Matlock DK (2004) Solid State Mat Sci 8:219
5. Bhadeshia HKDH, Christian JW (1990) Metall Trans 21A:767
6. Honeycombe RWK, Bhadeshia HKDH (1995) Steels microstructure and properties, 2nd edn. Edward Arnold, London
7. Mujahid S, Bhadeshia HKDH (1992) Acta Metall Mater 40:389
8. Hillert M, Hoglund L, Agren J (1993) Acta Metall Mater 41:1951
9. Van Dooren D, De Cooman BC, Thibaux P (2004) Proceedings of the international conference on advanced high strength sheet steels for automotive application, Warrendale. AIST, PA, pp 247
10. Agren J (1989) Acta Metall 37:181
11. Olson GB, Bhadeshia HKDH, Cohen M (1989) Acta Metall 37:381
12. Olson GB, Bhadeshia HKDH, Cohen M (1990) Metal Trans A 21A:805
13. Mujahid SA, Bhadeshia HKDH (1993) Acta Metall Mater 41:967
14. Wang J, Van Der Zwaag S (2001) Mettal Mater Trans A 32A:1527
15. Quidort D, Brechet YJM (2001) Acta Mater 49:4161
16. Christian JW, Edmonds DV, Marder AR, Goldstein JI (eds) (1984) TMS–AIME. Warrandale, PA, pp 293
17. Rees GI, Bhadeshia HKDH (1992) Mater Sci Tech 8:985
18. Hall DJ, Bhadeshia HKDH, WM Stobbs (1982) J de Phys, Colloque C4, No. 12 43:C4–449
19. Bhadeshia HKDH (1981) Proceedings of the international solid-solid phase transformations conference, Pittsburgh, p 1041